

Diffusion tensor imaging of the kidney at 3 Tesla MRI: normative values and repeatability of measurements in healthy volunteers

Bengi Gürses, Özgür Kılıçkesmez, Neslihan Taşdelen, Zeynep Fırat, Nevzat Gürmen

PURPOSE

To evaluate the feasibility of renal diffusion tensor imaging and determine the normative fractional anisotropy and apparent diffusion coefficient values at 3 Tesla magnetic resonance imaging (MRI) using parallel imaging and free breathing technique.

MATERIALS AND METHODS

A total of 52 young healthy volunteers with no history of renal disease were included in the study. MRI examinations were performed with 3 Tesla MRI equipment, using six-channel phased array SENSE Torso coil. In all subjects, T2-weighted turbo spin echo and diffusion tensor imaging using single shot echo planar imaging sequences were obtained in the coronal plane with free breathing. Field of view, slice thickness, and slice gap values were identical for both sequences for anatomic correlation during analysis of diffusion tensor imaging data. Parallel imaging method was used with a SENSE factor of 2. Diffusion tensor parameters of the cortex and medulla were determined and the intra- and inter-observer measurement variances were calculated.

RESULTS

The mean fractional anisotropy of the medulla was significantly higher than that of the cortex, whereas the mean apparent diffusion coefficient of the medulla was lower when compared with that of the cortex. According to the two-sided paired samples Student's *t* test, the intra- and inter-observer measurements correlated well.

CONCLUSION

This study shows the feasibility of renal diffusion tensor imaging and repeatability of diffusion tensor parameter measurements in 3 Tesla MRI.

Key words: • diffusion-weighted imaging • anisotropy • kidney

Magnetic resonance (MR) diffusion-weighted imaging (DWI) is capable of revealing the random motion of water molecules known as Brownian motion. DWI enables the measurement of tissue diffusion parameters *in vivo*. The main parameter derived from DWI is the apparent diffusion coefficient (ADC). The ADC is the water diffusion coefficient in tissues and is used to quantify the combined effects of capillary perfusion and diffusion *in vivo*. In freely moving fluids, the main factors affecting the ADC are temperature, molecular interactions, and tissue architecture. In contrast, the motion of protons in tissue structures is affected by a variety of factors including cellular density, membranes, and macromolecules. Thus, ADC is altered by various physiological and pathological conditions of organ systems. Because DWI has high motion sensitivity, this technique could only be applied initially in neuroimaging. Aided by ultra-fast pulse sequences such as echo-planar imaging (EPI), DWI has been made available for body imaging (1, 2) and has been used for imaging a variety of intra-abdominal organs including the prostate, liver, pancreas, adrenals, gastrointestinal system, and kidney to characterize focal lesions and diffuse parenchymal pathologies (2–4).

The kidney is a challenging organ for the application of DWI due to its high blood flow and water transport functions. In the literature, a limited number of clinical studies exist regarding kidney DWI in terms of the feasibility of imaging renal mass lesions and parenchymal pathologies. Significant alterations of kidney diffusion parameters have been shown in different pathological situations using DWI (5–7).

Diffusion is not a single-dimensional process, and in organized tissue structures, diffusion does not occur equally in all directions. In the kidneys, diffusion has anisotropic properties due to the presence of collecting ducts, tubules, and accompanying vessels that are oriented radially, especially in the medulla. Anisotropic properties of tissues can be best evaluated using diffusion tensor imaging (DTI), which, unlike DWI, allows the analysis of diffusion along multiple directions. DTI has been extensively used in neuroimaging to display various tracts and visualize the fiber organization of the brain. Aided by technical advances, the use of DTI is also possible for some of the abdominal viscera. High-field, 3 Tesla (T) MR imaging (MRI) systems provide an approximately two-fold increase in signal-to-noise ratio, higher resolution and improved image quality for the DTI technique. Similar to DWI, an EPI sequence is used for DTI. An increase in susceptibility artifacts has been overcome in 3 T systems by using a parallel imaging technology that aids in the reduction of echo spacing and echo train length (3, 5, 8). DTI was first applied to the kidneys of healthy volunteers by Ries et al. (9) using 1.5 T MRI equipment, and these authors demonstrated the anisotropic nature of the kidney by generating fractional anisotropy (FA) maps. A limited

From the Department of Radiology (B.G. ✉ bengur0@yahoo.com), Yeditepe University School of Medicine, İstanbul, Turkey.

Received 21 September 2010; revision requested 11 October 2010; revision received 15 October 2010; accepted 1 November 2010.

Published online 25 November 2010
DOI 10.4261/1305-3825.DIR.3892-10.1

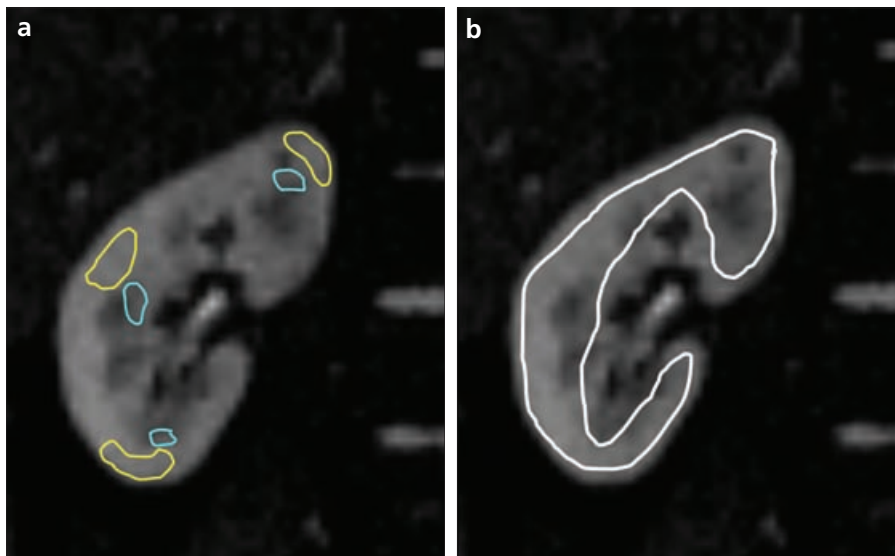


Figure 1. a, b. Free-hand ROIs placed separately at the cortex and medulla of the upper pole, mid-zone, and lower pole (a), and the global ROI placement including all of the cortex and medulla (b) are shown on the $b=0$ images.

number of studies have been published regarding DTI of the kidneys, and only one recently published study used a 3 T system (10). The aim of this study was to investigate the repeatability of kidney DTI measurements in healthy volunteers through intra- and inter-observer variability using 3 T equipment and parallel imaging technology.

Materials and methods

Study population

Fifty-four young healthy volunteers with no history of renal disease, previous renal surgery, diabetes, hypertension, or any systemic disease potentially involving the kidneys were included in the study. The study population consisted of 31 male and 23 female subjects with a mean age of 34 years (range, 24–41 years). The study was approved by the local ethics committee. Informed consent was obtained from each subject prior to the MRI examination. The mean duration of the procedure was 14.5 min. All of the MRI examinations were performed in the fasting state to minimize artifacts, and fluid intake was restricted directly before the examinations.

MRI

MRI examinations were performed using a 3 T scanner (Intera Achieva, Philips, Best, The Netherlands) equipped with high-performance gradients with a maximum strength of 80 mT/m and a slew rate of 200 mT/m/ms,

equipped with a six-channel phased array SENSE Torso coil. In all subjects, T2-weighted turbo spin echo (TSE) (slice thickness, 3 mm; number of slices, 40; NEX, 2; TR, 2729 ms; TE, 68 ms; matrix, 300×432; acquisition time, 3.44 min) and DTI using single shot echo planar imaging (ss-EPI) (slice thickness, 3 mm; TR, 10 000 ms; TE, 60 ms; matrix, 100×132; voxel size, 1.67×1.65×3.00 mm; acquisition time, 6.12 min; NEX, 2; number of slices, 40; b , 0 and 700 s/mm^2) sequences were obtained in the coronal plane during free breathing. The field of view (FOV), slice thickness and slice gap values were identical for both sequences to allow anatomical correlation during the analysis of the DTI data. The parallel imaging method was used with a SENSE factor of 2. The number of diffusion directions for the DTI sequence was 16.

DTI data analysis

Initially, DTI images were evaluated by one of the authors to decide whether the image quality was satisfactory for further analysis. In two subjects, there were intense motion artifacts, and these subjects were excluded from the study. For the remaining 52 subjects, no N/2 ghosting artifacts, eddy currents or significant distortions due to susceptibility were found. The DTI images of these subjects were accepted as having satisfactory image quality. All of the acquired datasets for the 52 subjects were transferred to the man-

ufacturer-supplied software (PRIDE) for analysis. FA maps, ADC maps, and color maps were produced. The T2-weighted images were reviewed for anatomical guidance to discriminate between the cortex and medulla.

Two separate, freehand regions of interest (ROIs) were placed on the cortex and medulla of the upper pole, mid-zone, and lower pole of each kidney in each patient; this was performed twice by one of the authors and once by another author experienced in genitourinary imaging and DTI measurements (Fig. 1a). The mid-coronal image was used during ROI placement. The mean FA and ADC values were determined for the cortex and medulla separately and compared between the two regions.

Statistical analysis was performed using Student's t-test, and P values of less than 0.05 were regarded as statistically significant. The inter- and intra-observer variations were determined using a two-sided, paired-samples Student's t-test. Tractography was performed using the streamlines fiber tracking algorithm. Anisotropy and angular thresholds were set in the range of 0.12–0.20 and 30–40°, respectively. The orientation of the kidney fibers in the cortex and medulla was evaluated using tractography. Red colors represented a right-left orientation, blue represents a cranio-caudal orientation, and green represents an antero-posterior orientation of diffusion. Changes in the intensity of the color represented different strengths of anisotropy.

The measurements were repeated using free hand ROI including the entire cortex and medulla (Fig. 1b), again by two different radiologists. The first radiologist measured the FA and ADC of all the kidneys from the mid-coronal image using free hand ROI twice to determine intra-observer variability, and the second radiologist performed the same measurements once to determine inter-observer variability. Intra- and inter-observer variability were calculated using a two-sided, paired-samples Student's t-test.

Results

Two subjects were excluded from the study due to intense motion artifacts. Therefore, 52 healthy volunteers were included in the DTI analysis. For each of these volunteers, the DTI image quality was satisfactory for further evaluation. The measurements are abbreviated as

follows: $ADC_{\text{first/first}}$ and $FA_{\text{first/first}}$ represent the first measurements of the first observer; $ADC_{\text{first/second}}$ and $FA_{\text{first/second}}$ represent the second measurements of the first observer; and ADC_{second} and FA_{second} represent the measurements of the second observer when ROIs are inserted separately in the cortex and medulla. The mean ADC value of the cortex was significantly higher compared to the mean ADC of the medulla for all three measurements ($P < 0.01$). Regarding FA values, the medulla was determined to be more anisotropic than the cortex. There was no significant difference among the FA and ADC values between the upper pole, mid-zone, and lower pole of the kidneys for all three measurements ($P > 0.05$).

For the cortex the mean $ADC_{\text{first/first}}$ ($\times 10^{-3} \text{mm}^2/\text{s}$) and $FA_{\text{first/first}}$ values were 2.22 ± 0.33 and 0.26 ± 0.05 , respectively, the mean $ADC_{\text{first/second}}$ and $FA_{\text{first/second}}$ values were 2.30 ± 0.29 and 0.27 ± 0.07 , respectively, and the mean ADC_{second} and FA_{second} values were 2.21 ± 0.48 and 0.24 ± 0.07 , respectively. For the medulla, the mean $ADC_{\text{first/first}}$ and $FA_{\text{first/first}}$ values were 1.99 ± 0.34 and 0.36 ± 0.11 , respectively, the mean $ADC_{\text{first/second}}$ and $FA_{\text{first/second}}$ values were 1.87 ± 0.44 and 0.34 ± 0.05 , respectively, and the mean ADC_{second} and FA_{second} values were 1.94 ± 0.32 and 0.33 ± 0.06 , respectively. For the ADC values of both the cortex and medulla, the two-sided,

paired-samples Student's t-test showed no significant difference between the first and second measurements of the first observer ($P = 0.089$ for cortex, $P = 0.083$ for medulla) and the measurements of the second observer ($P = 0.77$ for cortex, $P = 0.20$ for medulla). The FA values for the cortex and medulla also showed no significant difference between the first and second measurements of the first observer ($P = 0.81$ for cortex, $P = 0.50$ for medulla) and the measurements of the second observer ($P = 0.10$ for cortex, $P = 0.13$ for medulla). The mean ADC and FA values for all three measurements are provided in detail in Table 1.

The FA and ADC measurements were again made twice by the first and once by the second observer using the free hand ROI technique including the entire cortex and medulla, and these values were compared using the two-sided, paired-samples Student's t-test. The globally measured mean $FA_{\text{first/first}}$ was 0.28 ± 0.47 , the mean $FA_{\text{first/second}}$ was 0.29 ± 0.46 , and the mean FA_{second} was 0.28 ± 0.48 . There was no significant difference between the first and second FA measurements of the first observer ($P = 0.92$) and the measurements of the second observer ($P = 0.66$). The globally measured mean $ADC_{\text{first/first}}$ was 2.21 ± 0.22 , the mean $ADC_{\text{first/second}}$ was 2.22 ± 0.18 , and the mean ADC_{second} was 2.23 ± 0.17 . There was no significant dif-

ference between the first and second ADC measurements of the first observer ($P = 0.46$) and the measurements of the second observer ($P = 0.66$). The FA and ADC values from the global measurements and their P values are displayed in Tables 2 and 3. Figs. 2 and 3 show the graphs of FA and ADC values for all subjects from the global measurements.

After the repeatability of the DTI parameters was confirmed, tractography was performed using the manufacturer-supplied software and the streamlines fiber tracking algorithm. Tractography revealed a radially oriented direction of diffusion in the medulla that correlated well with the known ultrastructural features of the renal medulla (Fig. 4).

Discussion

Imaging of the kidney with DWI has been the subject of much interest in recent years since it became technically available for intra-abdominal organs. The kidney is unique in its major function, the transport of water, and its water content is higher than any other organ in the body. Water transport primarily occurs in the tubules and includes reabsorption, dilution, and concentration. The kidney can be regarded as a good candidate for the DWI technique due to the high blood flow and water transport that will affect the diffusion parameters. First, we performed feasibility studies using different ac-

Table 1. The mean FA and ADC values of each measurement from the cortex and medulla

	Cortex		Medulla	
	FA	ADC ($10^{-3} \text{mm}^2/\text{s}$)	FA	ADC ($10^{-3} \text{mm}^2/\text{s}$)
1st observer 1st measurement	0.26 ± 0.05	2.22 ± 0.33	0.36 ± 0.11	1.99 ± 0.34
1st observer 2nd measurement	0.27 ± 0.07	2.30 ± 0.29	0.34 ± 0.05	1.87 ± 0.44
2nd observer	0.24 ± 0.07	2.21 ± 0.48	0.33 ± 0.06	1.94 ± 0.32
Mean ^a	0.26 ± 0.06	2.26 ± 0.37	0.35 ± 0.07	1.93 ± 0.37

FA, fractional anisotropy; ADC, apparent diffusion coefficient

^a $P < 0.01$ for the difference between the mean FA and ADC values of the cortex and medulla

Table 2. The mean FA and ADC values with the global free-hand ROI from the first and second measurements of the first observer and the second observer

	FA	ADC ($10^{-3} \text{mm}^2/\text{s}$)
1st observer 1st measurement	0.28 ± 0.47	2.21 ± 0.22
1st observer 2nd measurement	0.29 ± 0.46	2.22 ± 0.18
2nd observer	0.28 ± 0.48	2.23 ± 0.17

FA, fractional anisotropy; ADC, apparent diffusion coefficient

Table 3. The P values derived from a two-sided, paired-samples Student's t-test

	FA	ADC
Intra-observer	0.92	0.46
Inter-observer	0.66	0.66

FA, fractional anisotropy; ADC, apparent diffusion coefficient

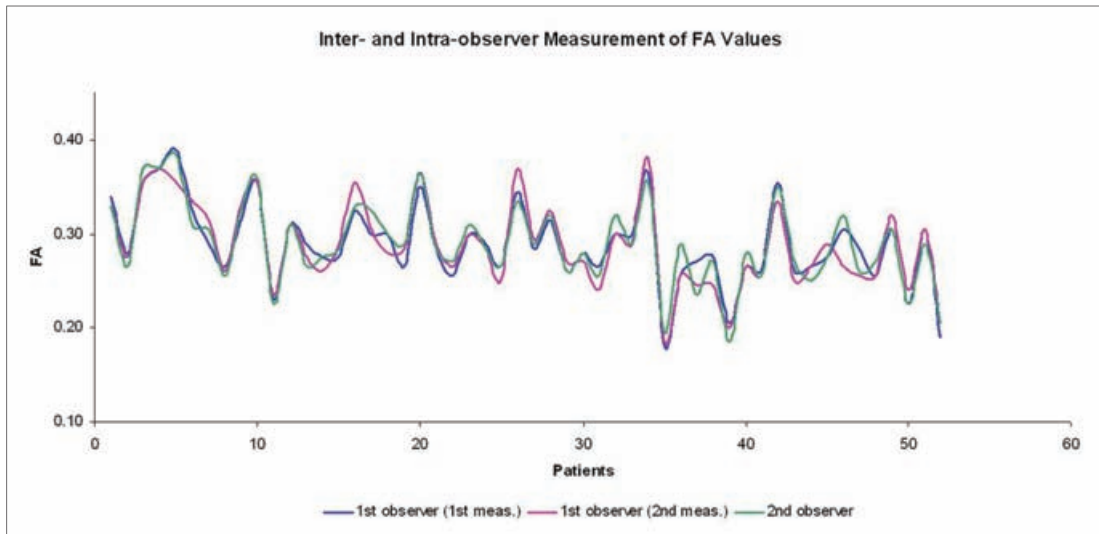


Figure 2. Graph showing the global FA values from the first and second measurements of the first observer and the measurements of the second observer.

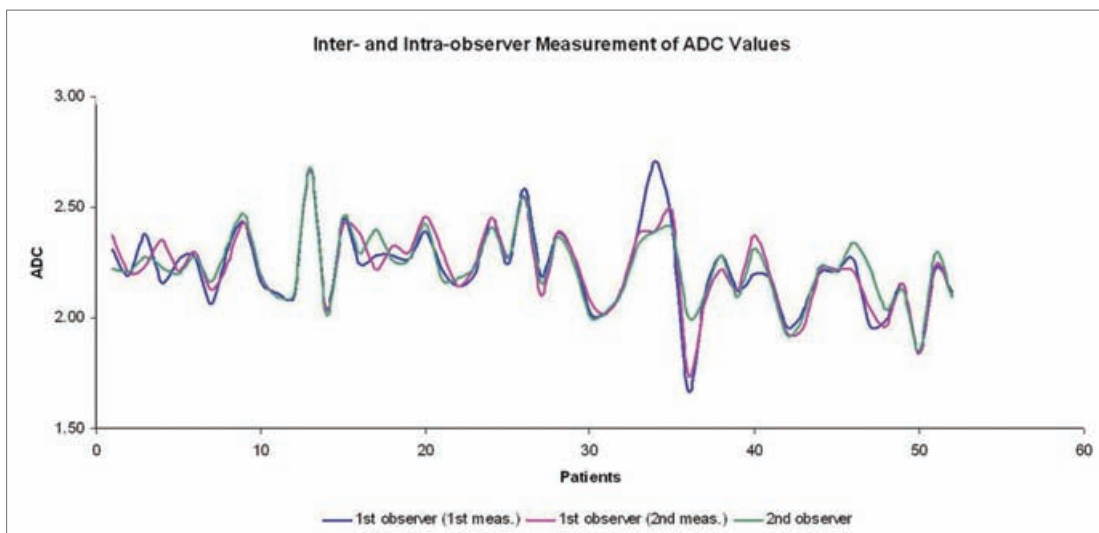


Figure 3. Graph showing the global ADC values from the first and second measurements of the first observer and the measurements of the second observer.

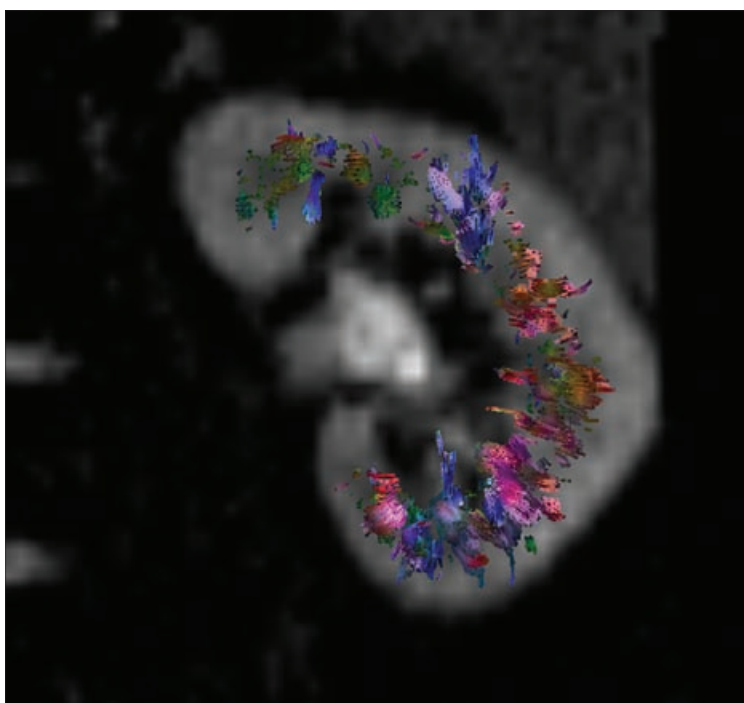


Figure 4. Tractography image showing the radial orientation of diffusion in the medulla. Red colors represent a right-left orientation, blue represents a cranio-caudal orientation and green represents an antero-posterior orientation of diffusion. Changes in the intensity of the color represent different strengths of anisotropy.

quisition parameters to show the repeatability of the DWI measurements and to optimize the technique (5, 11). Later, we investigated the possible role of kidney DWI for the identification of renal lesions and diffuse parenchymal diseases (5, 6, 12).

Thoeny et al. (5) performed DWI of the kidney in 18 healthy volunteers and in 15 patients with diffuse renal diseases. They used 1.5 T MRI and a variety of b values ranging from 0 to 1000 s/mm² with a free breathing technique and achieved satisfactory image quality; this is different from most studies of kidney DWI and DTI, which

have been performed with breath-hold or respiratory triggered techniques. We used a free breathing technique in our study similar to Thoeny et al. (5) and gained satisfactory results in terms of DTI image resolution. We propose that the use of a free breathing technique will enable diffusion MRI examination of kidneys in patients who are unable to cooperate with the breath-holding procedure. Hydration status is another important factor that may potentially affect the diffusion parameters. The results of a study by Müller et al. (11) showed decreased ADC values in the kidneys of dehydrated healthy volunteers that increased upon rehydration, and this difference was statistically significant. The increased ADC values after rehydration were attributed to the increase in glomerular filtration rate and increased osmotically driven water motion in the kidney. To decrease the inter-individual variation, fluid intake was restricted in our study prior to the MRI examination. Nevertheless, the relatively high inter-individual variations in the diffusion parameters of the kidney compared with other intra-abdominal parenchymal organs can be attributed in part to the inevitable difference in hydration status.

Diffusion-weighted MRI has been applied to a variety of pathologic renal conditions, including parenchymal diseases, vascular pathologies and focal lesions. Verswijvel et al. (6) demonstrated restricted diffusion in renal infection based on the ADC values. In a study by Namimoto et al. (13), ADC values were significantly decreased in acute and chronic renal failure (compared with normal subjects), and there was a linear correlation between the ADC value and serum creatinine level in the cortex. Yildirim et al. (12) observed decreased ADC values in the kidney in renal artery stenosis, and a strong correlation was detected between the ADC value and the degree of stenosis. DWI has also been used to evaluate renal allografts in transplant patients, and diffusion indices were reported to correlate significantly with serum creatinine concentrations (14). Most kidney DWI MRI studies have had promising results when using this technique for the functional evaluation of the kidneys. A limited number of studies exist regarding DWI in focal renal lesions (4, 15). In general, malignant and solid lesions have lower ADC

values than benign and cystic lesions. Kim et al. (15) found the lowest ADC values in angiomyolipoma and renal cell carcinoma in a study including a variety of focal renal lesions, including cysts.

DWI performed only in one direction can possibly result in the loss of important data in terms of the anisotropy for certain tissues. Basic anatomical components of the kidney such as the collecting tubules and ducts, which have an essentially radial orientation in the medulla, can be best evaluated using DTI, which (unlike DWI) is capable of detecting anisotropy through the analysis of diffusion along at least six directions. Initially, Ries et al. (9) applied DTI to the kidneys of 10 healthy volunteers using a 1.5 T MRI system and an ss-EPI sequence. The mean FA value of the cortex and medulla were found to be 0.22 ± 0.12 and 0.39 ± 0.11 , respectively, which show good correlation with our results. In 2008, Notohamiprodjo et al. (8) performed renal DTI using a 1.5 T system in healthy volunteers and patients with renal pathologies. In the healthy volunteers, consistent with the previous study and our results, the medulla was found to be more anisotropic with higher FA values than the cortex. The FA value of solid tumors was significantly higher than that of simple cysts, but renal cell carcinoma showed a wide range of FA values. In another study by Kataoka et al. (16), different parameters were applied for the optimization of renal DTI using 1.5 T MRI. Five sequences with different parameters including slice thickness, b values, respiratory triggered acquisition and multiple breath-holding were compared. Similar to our study, the FA of the cortex was found to be lower and the ADC higher than the medulla in all sequences. They used two b values (200 and 400 s/mm²) and observed that the higher b value was superior in accurately measuring diffusion and minimizing the effect of perfusion. ADC values show a decremental course with increased b values. When low b values are used (e.g., <100 s/mm²), ADC results are influenced by intravoxel coherent motion and are improved. In addition, it has been shown that the standard deviation in ADC values is greater when smaller b values are used (16). While deciding the b value in this study, we consid-

ered the ADC of the kidney. The optimal b value is calculated as: $1/(\text{ADC}) = b$ value, which is within 1% of the theoretical optimal value. From previous studies, the ADC of the normal kidney has been reported to have a spectrum from 3.00 to 1.50×10^{-3} mm²/s. With the above mentioned data, b values in the range of 300–700 s/mm² appear appropriate for renal DTI (3, 10). In a study by Thoeny et al. (5), when low b values were used for diffusion-weighted imaging, they found no significant difference between the ADC values of the cortex and the medulla in healthy kidneys; this result has been attributed to the effect of higher true diffusion in the cortex being counteracted by the greater anisotropy that results from the radial orientation of medulla structures. There was a significant difference among ADC values of the cortex and medulla in a high b value group (5). With high b values, the effect of perfusion is cancelled out, and the ADC value reflects mostly diffusion. The lack of a significant difference in ADC values with low b value has been attributed to the cancellation effect of the higher anisotropic features of the medulla over the 'true diffusion' in the cortex (10). For the above-mentioned reasons, the b value was selected to be 700 s/mm² in our study.

To decrease the acquisition time and artifacts associated with diffusion imaging, parallel imaging was used in this study. Parallel imaging also results in changes in the background signal intensity such that measurements of the signal-to-noise and contrast-to-noise ratios (SNR and CNR) would not be precise. For this reason, no such measurements were made in our study.

Modern 3 T MRI systems with higher SNR values are known to provide better spatial and temporal resolution and to allow DWI and DTI examinations to be completed in shorter time periods than in weaker magnetic field systems. Although susceptibility artifacts are theoretically increased, parallel imaging technology (used in our study) helps to overcome this problem and provides superior images. These technical advances have allowed for the acquisition of DTI in intra-abdominal organs with satisfactory image quality.

Recently, the feasibility of renal DTI with 3 T MRI has been studied by Notohamiprodjo et al. (10) in 10 volunteer subjects. The medulla was

found to be more anisotropic than the cortex, a finding consistent with previous studies. The volunteers were scanned using both 3 T and 1.5 T instruments, and the results were compared. According to the SNR and CNR measurements, they observed improved corticomedullary discrimination at 3 T, whereas the FA and ADC values were not significantly different. The inter-reader correlation was best when using a respiratory triggering technique rather than the breath-hold and free-breathing protocols.

There are some limitations of our study, the most important of which arises from the inevitable variations in the hydration status of patients. We have attempted to standardize this through water restriction before the MRI examination. Another important limitation is the use of a free-breathing protocol, but we believe that a demonstration of the feasibility of this technique will aid its application in patients who are unable to cooperate with breath holding protocols. Ideally, free-breathing and respiratory triggering techniques should have been compared in this study for complete optimization of the protocol for future studies.

Our study was aimed at showing the normative values and feasibility of renal DTI through intra- and inter-observer variance in a 3 T MRI system using the free-breathing protocol. To our knowledge, this study contains the largest series of renal DTI of healthy

volunteers performed in high magnetic field MRI and demonstrates a good correlation among readers.

In conclusion, kidney DTI performed with high magnetic field systems is feasible, and we believe that it is a promising tool for the evaluation of focal renal lesions and functional status of the kidney in diffuse parenchymal pathologies.

Conflict of interest disclosure

The authors declared no conflicts of interest.

References

1. Kim S, Naik M, Sigmund E, Taouli B. Diffusion-weighted MR imaging of the kidneys and the urinary tract. *Magn Reson Imaging Clin N Am* 2008; 16:585–596.
2. Koh DM, Collins DJ. Diffusion-weighted MRI in the body: applications and challenges in oncology. *AJR Am J Roentgenol* 2007; 188:1622–1635.
3. Gürses B, Tasdelen N, Yencilek F, et al. Diagnostic utility of DTI in prostate cancer. *Eur J Radiol* 2011; 79:172–176.
4. Kilickesmez O, Inci E, Atilla S, et al. Diffusion-weighted imaging of the renal and adrenal lesions. *J Comput Assist Tomogr* 2009; 33:828–833.
5. Thoeny HC, De Keyzer F, Oyen RH, Peeters RR. Diffusion-weighted MR imaging of kidneys in healthy volunteers and patients with parenchymal diseases: initial experience. *Radiology* 2005; 235:911–917.
6. Verswijvel G, Vandecaveye V, Gelin G, et al. Diffusion-weighted MR imaging in the evaluation of renal infection: preliminary results. *JBR-BTR* 2002; 85:100–103.
7. Damasio MB, Tagliafico A, Capaccio E, et al. Diffusion-weighted MRI sequences (DW-MRI) of the kidney: normal findings, influence of hydration state and repeatability of results. *Radiol Med* 2008; 113:214–224.
8. Notohamiprodjo M, Glaser C, Herrmann KA, et al. Diffusion tensor imaging of the kidney with parallel imaging: initial clinical experience. *Invest Radiol* 2008; 43:677–685.
9. Ries M, Jones RA, Basseau F, Moonen CT, Grenier N. Diffusion tensor MRI of the human kidney. *J Magn Reson Imaging* 2001; 14:42–49.
10. Notohamiprodjo M, Dietrich O, Horger W, et al. Diffusion tensor imaging (DTI) of the kidney at 3 tesla: feasibility, protocol evaluation and comparison to 1.5 Tesla. *Invest Radiol* 2010; 45:245–254.
11. Müller MF, Prasad PV, Bimmler D, Kaiser A, Edelman RR. Functional imaging of the kidney by means of measurement of the apparent diffusion coefficient. *Radiology* 1994; 193:711–715.
12. Yildirim E, Kirbas I, Teksam M, Karadeli E, Gullu H, Ozer I. Diffusion-weighted MR imaging of kidneys in renal artery stenosis. *Eur J Radiol* 2008; 65:148–153.
13. Namimoto T, Yamashita Y, Mitsuzaki K, Nakayama Y, Tang Y, Takahashi M. Measurement of the apparent diffusion coefficient in diffuse renal disease by diffusion-weighted echo-planar MR imaging. *J Magn Reson Imaging* 1999; 9:832–837.
14. Thoeny HC, Zumstein D, Simon-Zoula S, et al. Functional evaluation of transplanted kidneys with diffusion-weighted and BOLD MR imaging: initial experience. *Radiology* 2006; 241:812–821.
15. Kim S, Jain M, Harris AB, et al. T1 hyperintense renal lesions: characterization with diffusion-weighted MR imaging versus contrast-enhanced MR imaging. *Radiology* 2009; 251:796–807.
16. Kataoka M, Kido A, Yamamoto A, et al. Diffusion tensor imaging of kidneys with respiratory triggering: optimization of parameters to demonstrate anisotropic structures on fraction anisotropy maps. *J Magn Reson Imaging* 2009; 29:736–744.